Functionally Graded Stitched Laminates: Illustration on the Example of a Double Cantilever Beam

Victor Birman[1] and Larry W. Byrd[2]

Abstract: Although stitched laminates have been shown effective in preventing delamination failure, the presence of stitches results in a degraded in-plane strength and stiffness in such structures. The solution suggested in the paper is based on using stitches only in a part of the structure where they serve as arrestors of delamination cracks, while the part subject to considerable in-plane loading could remain unstitched. This approach, that could be called "functionally graded stitching," is considered on the example of a double cantilever beam (DCB) with a preexisting delamination crack that has penetrated into the stitched region of the beam. As is shown in the paper, the distribution of stitches in a functionally graded DCB (and in any other laminated structure) should be chosen to prevent three major failure modes. These modes include the failure of the stitches, bending failure of the unstitched delaminated section of the structure, and continuous crack propagation through the stitched region. The results obtained in the paper for the static problem clearly illustrate the feasibility of using functionally graded stitched laminates retaining in-plane strength and stiffness, while providing barriers to delamination cracks in less loaded regions of the structure. Additionally, the approach to the solution of the dynamic problem presented in the paper may be applied to the analysis of fatigue delamination cracks in partially stitched structures.

DOI: 10.1061/(ASCE)0893-1321(2006)19:4(217)

CE Database subject headings: Laminates; Beams; Cantilevers.

Introduction

Delamination cracking represents one of the most dangerous modes of failure in laminated composites. Stitching is a reliable method of reducing delamination tendencies since stitches effectively transform a plane or surface-constrained system of fibers into a three-dimensional system with enhanced strength and stiffness in the direction perpendicular to a delamination crack. Reviews of the issues related to applications of stitched composites have been published by Dow and Dexter (1997) and Dransfield et al. (1994). Examples of recent research on various aspects of stitched laminates can be found in the papers by Yavuz et al. (2005), Lau et al. (2004), Yeh et al. (2004), Chen et al. (2003), Jegley et al. (2001), and Gui and Li (2001).

The superior resistance to delamination cracking exhibited by stitched laminates can be attributed to their enhanced fracture toughness. For example, Dexter and Funk (1986) showed that the Mode I fracture toughness in Kevlar stitched laminates increases by a factor of 30 compared to the same laminates without stitching. Similar conclusions were obtained by Sankar and Sharma (1995). The result obtained by Chen et al. (2001) for medium and high density stitches in laminated composites was even more encouraging, reflecting a 45 times increase in Mode I fracture toughness. According to Farley et al. (1992), the compressive strength after impact (CAI) can be improved by a factor of two in stitched laminates, reflecting the fact that the loss of strength after impact is associated with the delamination that can be prevented by stitches. The corresponding increase in CAI observed by Sankar and Sharma (1995) was even larger, i.e., 400%.

In spite of advantages of stitched laminates in resisting delamination cracking, in-plane strength of such three-dimensional (3D) composites (not to be confused with CAI referred to above) is inferior to their 2D counterparts as was shown by Dexter and Funk (1986), Farley et al. (1992), and Reeder (1995). As follows from these studies the reduction in in-plane strength in stitched laminates can vary from 20 to 50%. This reduction in in-plane properties is attributed to a misalignment of fibers and fiber damage within the layers constituting the laminate as a result of stitching.

Obviously, it is desirable to avoid detrimental effects of stitching, while retaining the advantages associated with using this technique. The approach advocated in this paper is based on using functionally graded stitched panels. In such panels, strips consisting of several rows of stitches are distributed over the planform to prevent the propagation of delamination cracks (Fig. 1). While the in-plane strength and stiffness in the stitched regions may be compromised, they are retained in unstitched parts of the panel. Therefore, the design suggested in the paper represents a compromise combining the regions with enhanced in-plane strength and stiffness and reduced delamination resistance with the strips of reduced in-plane strength and stiffness and enhanced delamination resistance. It is anticipated that such an approach could produce structures with a sufficiently high resistance against in-plane damage and reduced delamination tendencies.

The present paper illustrates the potential enhancement of delamination resistance in partially stitched functionally graded

[1]Professor, Engineering Education Center, Univ. of Missouri-Rolla, One University Blvd., St. Louis, MO 63121 (corresponding author). E-mail: vbirman@umr.edu

[2]Air Force Research Laboratory, AFRL/VASM, Wright-Patterson Air Force Base, OH 45433.

Note. Discussion open until March 1, 2007. Separate discussions must be submitted for individual papers. To extend the closing date by one month, a written request must be filed with the ASCE Managing Editor. The manuscript for this paper was submitted for review and possible publication on July 27, 2005; approved on April 11, 2006. This paper is part of the ***Journal of Aerospace Engineering***, Vol. 19, No. 4, October 1, 2006. ©ASCE, ISSN 0893-1321/2006/4-217–226/$25.00.

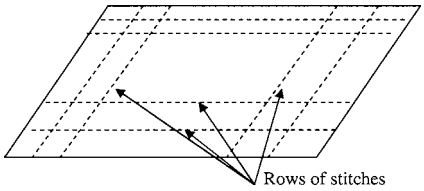

Fig. 1. Example of functionally graded stitched panel. Rows of stitches arrest delamination cracks, while avoiding reduction of in-plane strength and stiffness of most loaded central part.

laminates on the example of a double cantilever beam (DCB). DCB models have been used to demonstrate the effectiveness of stitched laminates by Sankar and Sharma (1995) and Dransfield et al. (1998), i.e., this is an accepted methodology of the analysis of such structures. However, contrary to the previous investigations, the present study is concerned with partially stitched beams. The solution is obtained exactly, accounting for transverse shear effects that become prominent in the case of short cracks. Both static as well as dynamic problems are considered. The solution of the former problem elucidates the effect of partial stitching on Mode I delamination cracks in the framework of standard DCB testing. The latter problem illustrates this effect in application to dynamic loading.

Static Analysis

Consider a DCB with a pre-existing delamination crack shown in Fig. 2. The beam is partially stitched and it is assumed that the crack initiated in the unstitched section and propagated to some extent into the stitched section of the beam. In this case, three modes of failure are possible:

1. The crack continues propagation into the stitched section. In the case where stitches are located only in a part of the beam and the crack that "unzipped" the stitched section emerges into the adjacent unstitched region, failure is practically unavoidable;
2. The stitches fail, beginning with the row adjacent to the unstitched region, i.e., at $x=c$. This will probably lead to the overall failure of DCB; and
3. The delaminated "legs" of the unstitched region fail due to bending. The paper presents the analysis that enables us to consider all three modes of failure.

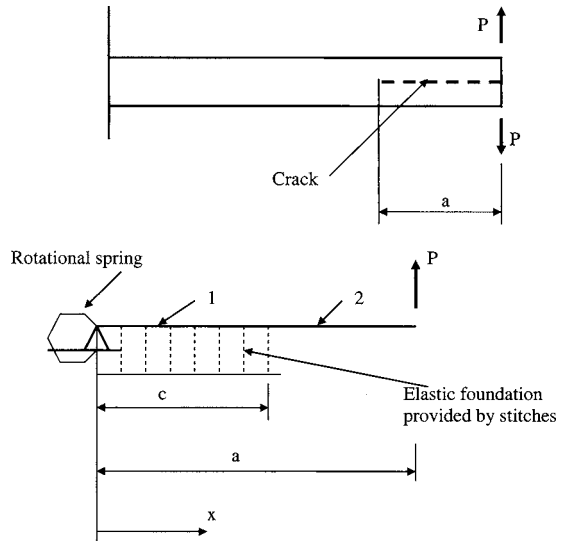

Fig. 2. Double cantilever beam used in Mode I fracture testing and model of leg of delaminated section adopted in analysis. In text, subsection 1 refers to stitched section $0 \leqslant x \leqslant c$ and subsection 2 is unstitched section $c \leqslant x \leqslant a$.

The pressure applied by the stitches to the delaminated legs of DCB was analyzed by Jain and Mai (1994) and Mabson and Deobald (2000). The analysis was conducted by the assumption that the stitches pass through the entire depth of DCB, loop over its surface, and connect to each other. As was shown in the latter paper, the reaction of stitches can be represented in the form resembling the reaction of a linear elastic foundation, i.e.

$$p = kw = \frac{\sigma_{\text{crit}} E_s r V_p b}{L(\sigma_{\text{crit}} r - \tau L)} w \tag{1}$$

The delaminated part of DCB within $0 \leqslant x \leqslant a$ can be analyzed as a beam supported by an elastic foundation with the modulus defined in Eq. (1) within the section $0 \leqslant x \leqslant c$. Transverse shear that can be important if the length of either stitched or unstitched section is relatively small compared to its depth is accounted for in the following analysis. The equations of equilibrium for the thick (shear-deformable) stitched section are (Korotkin et al. 1968)

$$EIw_b'' = M(x)$$

$$V(x) = -GAw_s'$$

$$\text{where } (\ldots)' = d(\ldots)/dx. \tag{2}$$

In homogeneous cross sections, the shear correction factor is often introduced to match the results obtained by the exact solutions of the theory of elasticity with the results obtained by the beam theory. Another approach to the evaluation of the shear correction factor involves matching the strain energies of the structure derived from the representative solutions. While detailed discussions of such analyses can be found elsewhere (see for example, Whitney 1987), typical values of the shear correction factor are 5/6 or 2/3, so that using the first value, $GA \rightarrow 5/6GA$. Accordingly, in the following, the shear stiffness of DCB is defined as $S=5/6GA$.

Following a standard chain of transformation, the bending moment in the right side of the first Eq. (2) is determined from the free-body diagram and this equation is differentiated twice yielding

$$EIw_b^{iv} + k(w_b + w_s) = 0 \tag{3}$$

Combining Eq. (2), expressing the derivative of the deflection due to transverse shear in terms of the third derivative of the bending deflection and integrating this expression produce

$$w_s = -\frac{EI}{S} w_b'' + f \tag{4}$$

where f=constant of integration.

The resulting equation of bending obtained from Eqs. (3) and (4) becomes

$$EIw_b^{iv} + kw_b - \frac{kEI}{S}w_b'' = -kf \tag{5}$$

The same equation could be derived following the approach presented by Yavari et al. (2001).

It is easy to observe that $w_b=-f$ being a particular integral of Eq. (5), the total deflection of the leg, i.e., $w=w_b+w_s$, does not depend on the constant of integration f. Accordingly, this constant can be set equal to zero. In this case, Eq. (5) becomes similar to the equation for a shear deformable beam resting on the elastic foundation.

The solution of Eq. (5) for the unstitched section of DCB, i.e., within $c \leqslant x \leqslant a$, (section 2 in Fig. 2) is

$$w_{b2} = A_1 + A_2x + A_3x^2 + A_4x^3 \tag{6}$$

where A_i=constants of integration.

Within the stitched region of the beam, i.e., $0 \leqslant x \leqslant c$, (section 1 in Fig. 2) the solution of Eq. (5) yields

$$w_{b1} = C_1F_1(x) + C_2F_2(x) + C_3F_3(x) + C_4F_4(x) \tag{7}$$

where C_i=constants of integration and functions $F_i(x)$ depend on the value of

$$\beta = \frac{1}{2S}\sqrt{kEI} \tag{8}$$

In particular, disregarding a seldom case where $\beta=1$, these functions are (Korotkin et al. 1968)

$$0 < \beta < 1$$

$$F_1(x) = \cosh \delta x \cos \gamma x \quad F_2(x) = \cosh \delta x \sin \gamma x$$

$$F_3(x) = \sinh \delta x \cos \gamma x \quad F_4(x) = \sinh \delta x \sin \gamma x \tag{9}$$

and

$$\beta > 1$$

$$F_1(x) = \cosh px \quad F_2(x) = \sinh px$$

$$F_3(x) = \cosh tx \quad F_4(x) = \sinh tx \tag{10}$$

where

$$\delta = \alpha\sqrt{1+\beta} \quad \gamma = \alpha\sqrt{1-\beta}$$

$$p = \alpha\sqrt{2(\beta + \sqrt{\beta^2-1})} \quad t = \alpha\sqrt{2(\beta - \sqrt{\beta^2-1})}$$

$$\alpha = \sqrt[4]{\frac{k}{4EI}} \tag{11}$$

The solution should satisfy the boundary conditions at the cross section corresponding to the tip of the delamination crack, i.e., at $x=0$, at the free end, i.e., at $x=a$, and the continuity conditions at the boundary of the stitched and unstitched regions, i.e., at $x=c$. Note that extensive studies of DCB (without stitches) illustrated that it is necessary to account for a limited rotational restraint of the intact part of the beam at the cross section $x=0$. The solutions accounting for such restraint using an elastic foundation approach in the intact part of DCB were first published in the case of isotropic beams by Kanninen (1973), for transversely isotropic materials by Williams (1989), and for angle-ply laminates by Ozdil and Carlsson (1999). An alternative approach, accounting for the rotational restraint through the analysis of the strain energy accumulated in the intact section of DCB as a result of the moment applied at $x=0$, was considered by Birman and Byrd (2005). As was shown in this paper, an accurate prediction of the coefficient of elastic restraint at $x=0$ can be given by the simple formula

$$K = \frac{\pi h^2 b}{8}\sqrt{Q_{11}Q_{55}} \tag{12}$$

where Q_{ii}=average reduced stiffnesses of the beam material. In the case where all layers are unidirectional and identical or if the material is plain woven, these stiffnesses are particularly easy to calculate being $Q_{11}=E_x/1-v_{xz}v_{zx}$, $Q_{55}=G_{xz}$ (standard notations for the moduli and Poisson's ratios in laminated composites are employed). Eq. (12) can also be used for a balanced cross-ply laminate with numerous layers using averaged values of reduced stiffnesses.

The boundary conditions at $x=0$ are

$$M(x=0) = EIw_{b1}'' = Kw_{b1}'$$

$$w_1 = w_{b1} + w_{s1} = 0 \tag{13}$$

Hereafter the subscripts "1" and "2" refer to the stitched and unstitched sections of DCB, respectively.

Using Eq. (4), the second condition (13) becomes

$$w_{b1} - \frac{EI}{S}w_{b1}'' = 0 \tag{14}$$

The boundary conditions at $x=a$ imply that

$$M(x=a) = EIw_{b2}'' = 0$$

$$w_{b2}''' = -\frac{P}{EI} \tag{15}$$

The second condition (15) follows from the requirement that the transverse shear force should be equal to the applied force and from Eq. (4).

Finally, the continuity conditions at $x=c$ are

$$w_1 = w_2 \quad w_1' = w_2'$$

$$M_1(x=c) = M_2(x=c) \quad V_1(x=c) = V_2(x=c) \tag{16}$$

It is easy to check that conditions (16) are satisfied if

$$w_{b1} = w_{b2} \quad w_{b1}' = w_{b2}'$$

$$w_{b1}'' = w_{b2}'' \quad w_{b1}''' = w_{b2}''' \tag{17}$$

Eight constants of integration in Eqs. (6) and (7) are determined from eight Eqs. (13)–(15) and (17).

It is noted that the presence of stitches may affect the values of the effective bending and shear stiffnesses of DCB. These effects can be accounted for by using the adjusted values of EI and S in the stitched sections.

As follows from numerical examples discussed below, the length of the unstitched section of DCB cannot be too large since in the absence of "support" provided by stitches excessive bending of the delaminated legs of DCB will likely result in failure. One possible solution is using a variable stitch volume fraction, combining sections with a low density of stitches (where in-plane strength and stiffness are mostly retained but a limited enhancement of delamination resistance is also achieved) with sections with a higher stitch density. Even if delamination cracks originate in the former sections, they would be arrested in the latter sec-

J. Aerosp. Eng., 2006, 19(4): 217-226

tions of the structure. For example, if DCB includes n sections with the stitch volume fraction V_{pi} in the ith section, the solution outlined above is applicable. In this case, the stiffness of the equivalent elastic foundation supporting the ith section, i.e., k_i, is obtained from Eq. (1) using the appropriate stitch volume fraction. The solution Eq. (7) for the ith stitched section is

$$w_{bi} = C_{1i}F_{1i}(x) + C_{2i}F_{2i}(x) + C_{3i}F_{3i}(x) + C_{4i}F_{4i}(x) \tag{18}$$

where functions F_{ji} depends on

$$\beta_i = \frac{1}{2S}\sqrt{k_i EI} \tag{19}$$

Eqs. (9)–(11) are modified accordingly for each stitched section of DCB.

Boundary conditions (13) and (14) remain without change if the first section is adjacent to the intact part of DCB. Conditions (15) have to be modified by replacing $w_{b2} \rightarrow w_{bn}$. The continuity conditions between the ith and $(i+1)$th regions are similar to Eq. (17)

$$w_{bi} = w_{b(i+1)} \quad w'_{bi} = w'_{b(i+1)}$$

$$w''_{bi} = w''_{b(i+1)} \quad w'''_{bi} = w'''_{b(i+1)} \tag{20}$$

Constants of integration being determined from the previous solution, it remains to specify the delamination arrest criterion. The approach to the problem adopted in this paper is similar to the method introduced by the authors for z-pinned structures (Birman and Byrd 2005). If the crack becomes longer, the characteristic crack opening defined as a separation of the delaminated legs of DCB at $x=a$ should increase as well. Therefore, if a longer crack does not result in a larger $w(a)$, we can assume that the crack is arrested since such a situation is physically impossible. Mathematically, the crack arrest phenomenon can be identified with the condition

$$\frac{dw(a)}{da} = 0 \tag{21}$$

Although the analytical evaluation of the derivative in Eq. (21) is impractical, this condition is easily detected from the curves $w(a)$ versus a available from the solution.

Dynamic Analysis

Besides enhancing the static delamination resistance, stitching the entire structure or its sections may be beneficial for the prevention of delamination fatigue damage. The approach to the solution of this problem is illustrated here for the case where vibrations of DCB are excited by the periodic force $P \sin \omega t$ applied to the upper leg (Fig. 3). The solution is obtained using a modification of the analysis of shear-deformable laminated beams (see for example, Reddy 2004).

Equations of motion of a section of DCB supported by stitches written by assumption that damping is negligible and based on the first-order shear deformation theory are

$$S(W_{i'xx} + \Phi_{i'x}) + \omega^2 I_0 W_i + kW_i = 0$$

$$EI\Phi_{i'xx} - S(W_{i'x} + \Phi_i) + \omega^2 I_2 \Phi_i = 0 \tag{22}$$

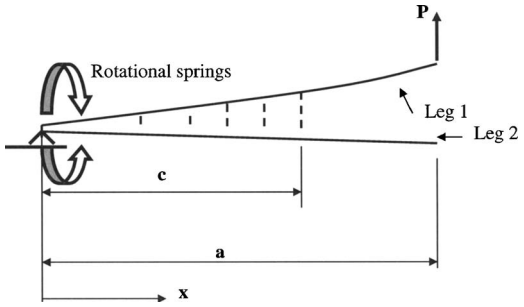

Fig. 3. Model of double cantilever beam considered for dynamic Mode I test. Delaminated legs are identified as Leg 1 (upper leg) and Leg 2 (lower leg).

where i identifies the upper ($i=1$) or lower ($i=2$) leg of the stitched section of the beam. The amplitudes of the deflection and rotation in Eq. (22) are related to the corresponding dynamic terms by

$$w_i(x,t) = W_i(x)\sin \omega t$$

$$\phi_i(x,t) = \Phi_i(x)\sin \omega t \tag{23}$$

The inertial terms in Eq. (22) are given by

$$\{I_0, I_2\} = b\int_{-h/2}^{h/2} \rho\{1, z^2\}dz \tag{24}$$

The substitution of the derivative of the amplitude of rotation from the first Eq. (22) into the differentiated second equation yields

$$\Phi_{i'x} = -W_{i'xx} - \frac{k}{S}W_i - \omega^2\frac{I_0}{S}w_i$$

$$EIW_{i'xxxx} + \left(\frac{EI\omega^2 I_0}{S} + \omega^2 I_2 + \frac{EIk}{S}\right)W_{i'xx} + \left[k\left(\frac{\omega^2 I_2}{S} - 1\right) - \omega^2 I_0 + \frac{\omega^4 I_0 I_2}{S}\right]W_i = 0 \tag{25}$$

The solution of the second Eq. (25) yields

$$W_i = \sum_{j=1}^{4} C_{ij}F_j(x) \tag{26}$$

where C_{ij}=unknown coefficients and $F_{ij}(x)$=functions evaluated for a particular geometry and material properties that are omitted here for brevity.

For unstitched sections, $k=0$ and the second Eq. (25) is reduced to the equation for a vibrating shear deformable beam derived by Reddy (2004) with the solution

$$W'_i = A_{i1}\sin \lambda_i x + A_{i2}\cos \lambda_i x + A_{i3}\sinh \mu_i x + A_{i4}\cosh \mu_i x \tag{27}$$

where A_{ij}=constants of integration. The expressions for λ_i and μ_i are given by Reddy (2004). The prime is used in Eq. (27) to distinguish deformations of the unstitched section from those of the stitched counterpart.

The amplitude of rotation $\Phi_i(x)$ can be determined from the second Eq. (22) substituting $\Phi_{i'xx}$ from the first Eq. (25). Therefore, there are 16 constants of integration that can be determined from 16 boundary and continuity conditions listed below

$$x = 0$$

$$W_1 = W_2 = 0, \quad M_i = EI\Phi_{i'x} = K\Phi_{i'x}$$

$$x = a$$

$$M_i = EI\Phi'_{i'x} = 0, \quad V_1 = S(W'_{1'x} + \Phi'_1) = -P$$

$$V'_2 = S(W'_{2'x} + \Phi'_2) = 0$$

$$x = c$$

$$W_i = W'_i, \quad \Phi_i = \Phi'_i, \quad M_i = M'_i, \quad V_i = V'_i \tag{28}$$

Given the amplitude and frequency of loading, the characteristic crack opening $\delta = W'_1(a) - W'_2(a)$ can be obtained as a function of the crack length. Similar to the static case, the crack arrest should be identified with condition (21).

Numerical Examples

The following examples illustrating the feasibility of partially stitched laminates are presented for two composite material systems, including a balanced graphite/epon resin beam (Ghate et al. 2004) and a unidirectional AS4-3501-6 graphite–epoxy. The thickness of the delaminated leg of DCB was taken equal to 2 mm, except for the cases shown in Figs. 14 and 15. The width of DCB was chosen equal to 22 mm.

The stiffness of the elastic foundation was estimated using typical stitch material properties, such as Kevlar yarn (Ghate et al. 2004) with the modulus of elasticity equal to 151.68 GPa or Kevlar-29 (Chen et al. 2001) with the modulus of 83.0 GPa (the effective modulus of a stitch is smaller than the values for single fibers listed above). The use of formula (1) requires us to specify a number of parameters, such as the stitch radius, the interfacial shear strength, the length of the stitch, and the stitch volume fraction. Based on available data, it can be predicted that the effective stiffness of the elastic foundation usually varies in the range from 10^8 to 10^{11} Pa. For example, consider the range of the stitch stiffness from 50 to 120 GPa, the stitch areal density or volume fraction between 0.1 and 1.5%, the length of the stitch between 5 and 10 mm, and the coefficient

$$k' = 1 - \frac{\tau}{\sigma_{\text{crit}}}\frac{L}{r} \tag{29}$$

varying from 0.1 to 1.0. In the prescribed ranges of these parameters, the effective stiffness of the elastic foundation for a 22-mm-wide DCB varies from 1.1^*10^8 to 7.9^*10^{10} Pa.

The accuracy of the solution was checked through a successful comparison of the deflections of the free end of DCB with a negligible stiffness of stitches to the results available in the literature for unstitched DCB beams. Furthermore, a comparison of the crack opening in a fully stitched DCB was in good agreement with the result shown in Fig. 6 of the paper by Dransfield et al. (1998) for a DCB prior to failure of stitches.

The effect of full stitching on the delamination crack opening in a representative DCB is shown in Figs. 4 and 5. As is observed in these figures, the deflection of the free end of a delaminated DCB without stitches rapidly increases with the length of the delamination crack. In both figures, this deflection exceeds the thickness of the delaminated section, even before the crack reaches the length of 30 mm. The presence of a very compliant elastic foundation corresponding to an extremely low volume fraction of stitches ($k=2^*10^7$ Pa) reduces the delamination tendency, but the arrest of the crack cannot be achieved in this case. However, a stiffer foundation ($k=4^*10^8$ Pa) results in an almost immediate arrest of the crack, even when it is very short (as discussed above, the arrest of the crack is identified with the horizontal deflection–crack length curve).

Both the effect of the stiffness of the effective elastic foundation provided by stitches as well as the influence of a degree of crack penetration into the stitched section of DCB are shown in

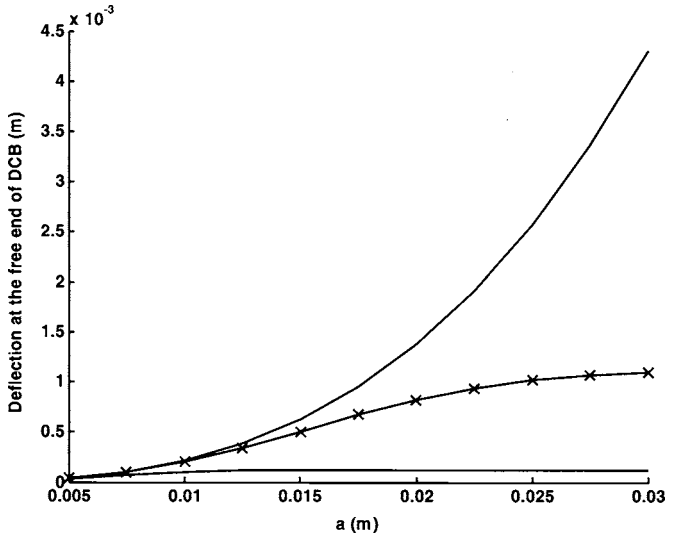

Fig. 4. Effect of presence of stitches on deflections of free end of fully stitched DCB specimen. Applied force is 200 N. Material of DCB is balanced graphite/epon resin laminate. Curves correspond to unstitched DCB (solid curve), $k=2^*10^7$ N/m^2 (-x-x-x-), and $k=4^*10^8$ N/m^2 (….).

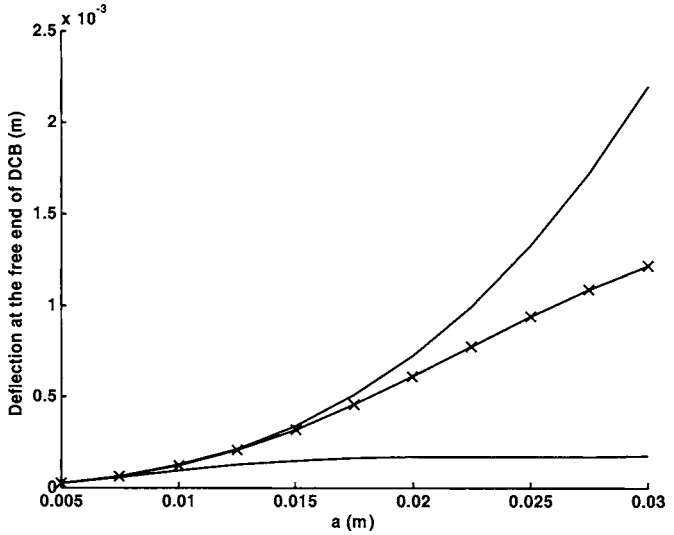

Fig. 5. Effect of presence of stitches on deflections of free end of fully stitched DCB specimen. Applied force is 400 N. Material of DCB is unidirectional AS4-3501-6 laminate. Curves correspond to unstitched DCB (solid curve), $k=2^*10^7$ N/m^2 (-x-x-x-), and $k=4^*10^8$ N/m^2 (….).

J. Aerosp. Eng., 2006, 19(4): 217-226

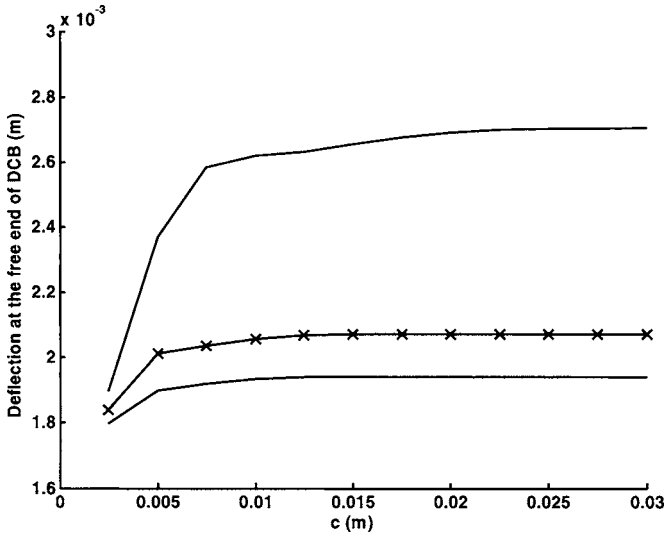

Fig. 6. Effect of length of stitched section of DCB and stiffness of elastic foundation provided by stitches on crack opening in graphite/epon DCB. Applied force is 200 N, length of unstitched section is 20 mm. Stiffness of foundation is equal to $k=10^9$ N/m^2 (solid curve), $k=6^*10^9$ N/m^2 (-x-x-x-), and $k=1.1^*10^{10}$ N/m^2 (….).

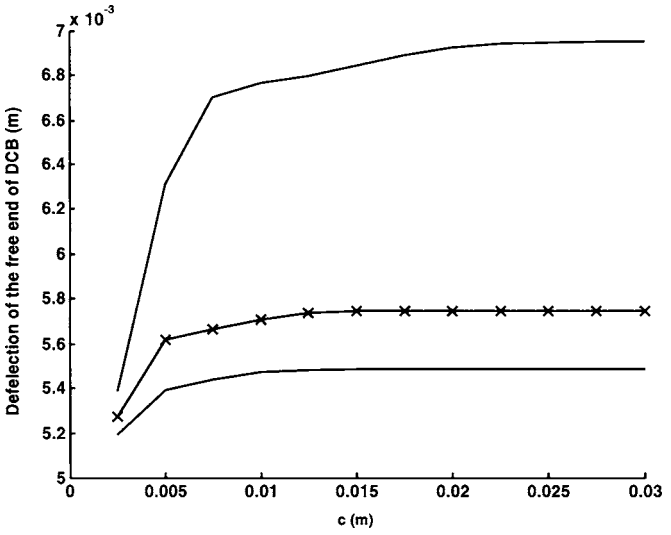

Fig. 8. Effect of length of stitched section of DCB and stiffness of elastic foundation provided by stitches on crack opening in graphite/epon DCB. Applied force is 200 N, length of unstitched section is 30 mm. Stiffness of foundation is equal to $k=10^9$ N/m^2 (solid curve), $k=6^*10^9$ N/m^2 (-x-x-x-), and $k=1.1^*10^{10}$ N/m^2 (….).

Figs. 6–9 for a graphite/epon beam and in Figs. 10–13 for an AS4-3501-6 beam. In particular, a stiffer foundation provided by stitches drastically reduces the deflection of the delaminated end of the crack as can be observed in Figs. 6, 8, 10, and 12. Moreover, the arrest of the crack supported by a stiffer foundation occurs at a smaller length of its penetration into the stitched section. In other words, by using stiffer stitches or increasing their density, it is possible to reduce the width of stitched sections of the structure. Predictably, a longer crack (longer delaminated sections unsupported by stitches) results in larger maximum deflections as follows from the comparison of Figs. 6, 8, 10, and 12. However, the length of a delaminated section of DCB unsupported by stitches does not affect the requirements that have to be satisfied for the arrest of the crack that depends only on the stiffness and density of the stitches and the width of the stitched section, i.e., the dimension c.

The failure of stitches and microbuckling or the loss of strength of DCB are two possible modes of failure, besides fracture. While the arrest of the crack can be achieved using a sufficiently stiff stitching system, the analysis of failure of the stitches requires us to estimate their strain. The results shown in Figs. 7, 9, 11, and 13 illustrate the elongation of the first row of stitches

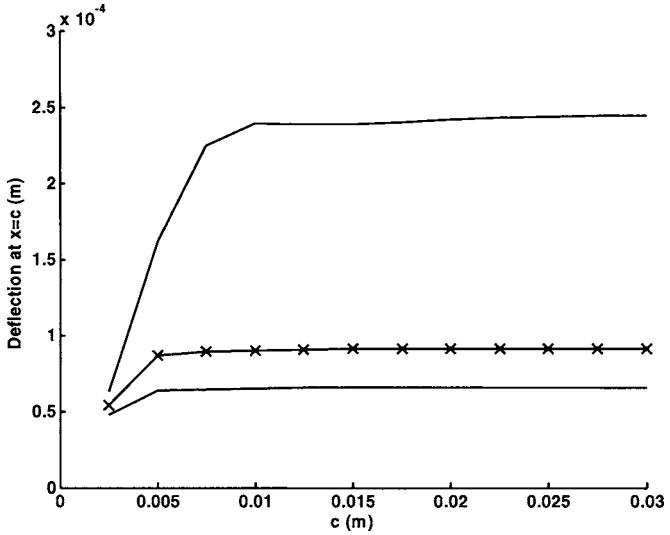

Fig. 7. Effect of length of stitched section of DCB and stiffness of elastic foundation provided by stitches on elongation of first row of stitches in graphite/epon DCB. Applied force is 200 N, length of unstitched section is 20 mm. Stiffness of foundation is equal to $k=10^9$ N/m^2 (solid curve), $k=6^*10^9$ N/m^2 (-x-x-x-), and $k=1.1^*10^{10}$ N/m^2 (….).

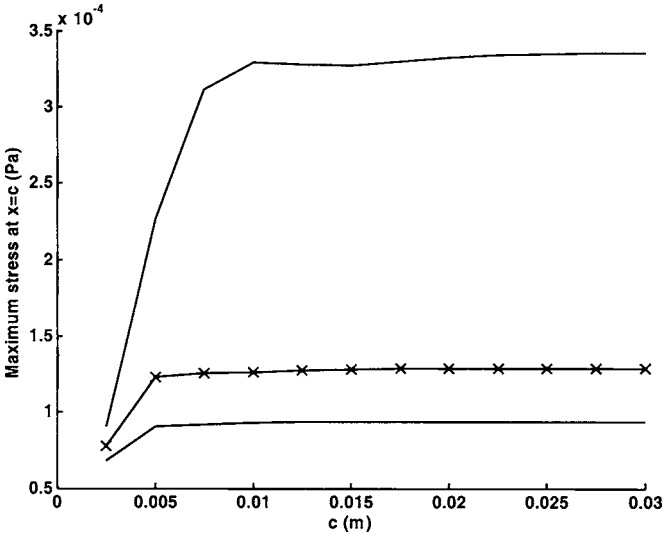

Fig. 9. Effect of length of stitched section of DCB and stiffness of elastic foundation provided by stitches on elongation of first row of stitches in graphite/epon DCB. Applied force is 200 N, length of unstitched section is 30 mm. Stiffness of foundation is equal to $k=10^9$ N/m^2 (solid curve), $k=6^*10^9$ N/m^2 (-x-x-x-), and $k=1.1^*10^{10}$ N/m^2 (….).

J. Aerosp. Eng., 2006, 19(4): 217-226

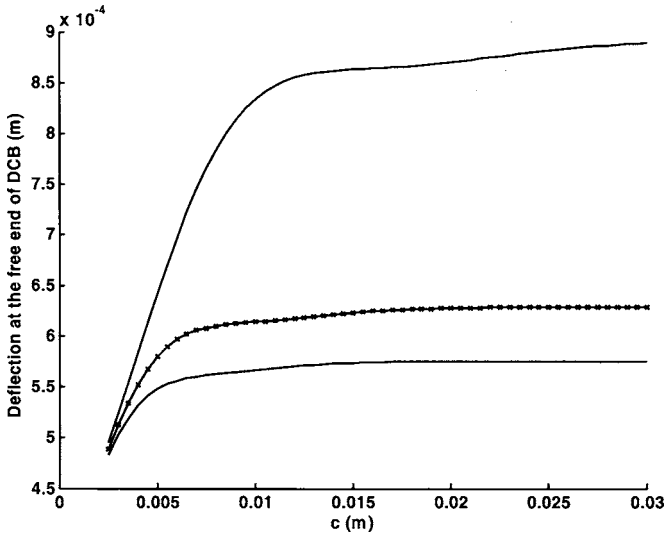

Fig. 10. Effect of length of stitched section of DCB and stiffness of elastic foundation provided by stitches on crack opening in unidirectional AS4-3501-6 laminated DCB. Applied force is 200 N, length of unstitched section is 20 mm. Stiffness of foundation is equal to $k=10^9$ N/m^2 (solid curve), $k=6^*10^9$ N/m^2 (-x-x-x-), and $k=1.1^*10^{10}$ N/m^2 (….).

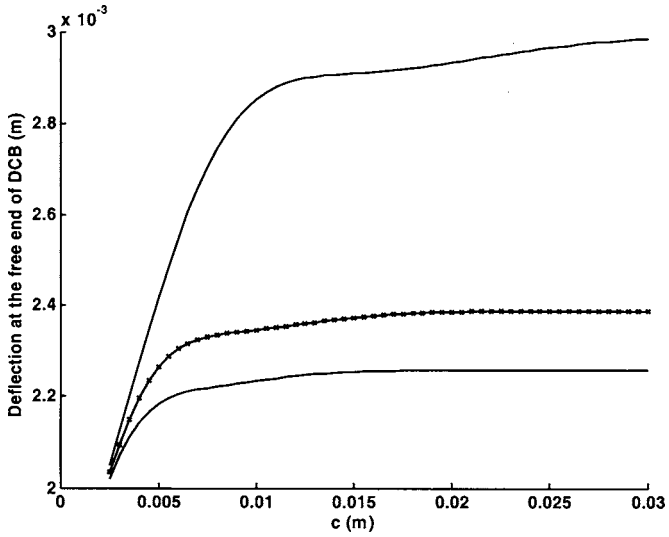

Fig. 12. Effect of length of stitched section of DCB and stiffness of elastic foundation provided by stitches on crack opening in unidirectional AS4-3501-6 laminated DCB. Applied force is 200 N, length of unstitched section is 35 mm. Stiffness of foundation is equal to $k=10^9$ N/m^2 (solid curve), $k=6^*10^9$ N/m^2 (-x-x-x-), and $k=1.1^*10^{10}$ N/m^2 (….).

adjacent to the unstitched section of DCB. It is observed that the pattern of the relationship between the length of the crack propagation into the stitched section versus deflections is similar for the deflections of the free end of DCB and the deflections of the first row of stitches, although the latter deformations are significantly smaller. As soon as the crack is arrested, i.e., condition (21) is satisfied, the elongation of the first row of stitches is also stabilized, i.e., $dw(c)/da=0$. The elongation of the stitches increases with an increase in the length of the unstitched section of DCB, as could be anticipated.

A better understanding of the danger of an excessive elongation in realistic stitched composites can be achieved considering the failure strain of the stitches and comparing it to the strain corresponding to deformations in Figs. 7, 9, 11, and 13. For example, the tensile strength of Kevlar 29 is 3.8 GPa (Barbero 1999). This implies the failure strain of 0.045 and the failure deformation of a 7 mm long stitch equal to 3.15^*10^{-4} m. Such deformations are observed for a lightly supported leg of DCB in Fig. 9. This estimate illustrates that failure of stitches should not be disregarded in the analysis of a partially stitched structure.

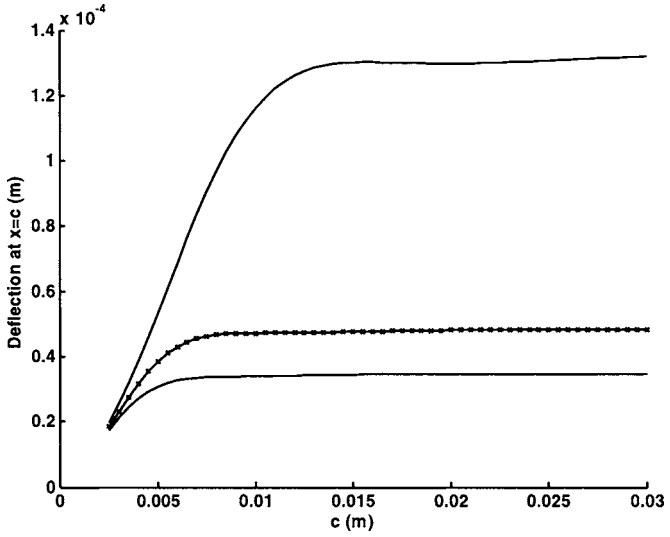

Fig. 11. Effect of length of stitched section of DCB and stiffness of elastic foundation provided by stitches on elongation of first row of stitches in unidirectional AS4-3501-6 laminated DCB. Applied force is 200 N, length of unstitched section is 20 mm. Stiffness of foundation is equal to $k=10^9$ N/m^2 (solid curve), $k=6^*10^9$ N/m^2 (-x-x-x-), and $k=1.1^*10^{10}$ N/m^2 (….).

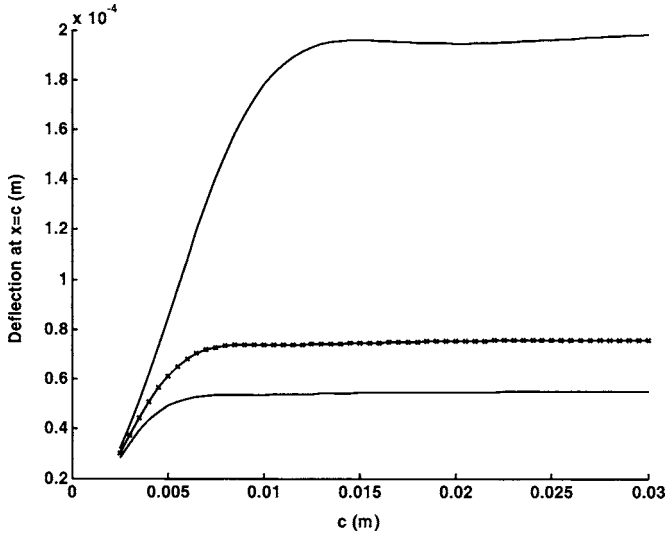

Fig. 13. Effect of length of stitched section of DCB and stiffness of elastic foundation provided by stitches on elongation of first row of stitches in unidirectional AS4-3501-6 laminated DCB. Applied force is 200 N, length of unstitched section is 35 mm. Stiffness of foundation is equal to $k=10^9$ N/m^2 (solid curve), $k=6^*10^9$ N/m^2 (-x-x-x-), and $k=1.1^*10^{10}$ N/m^2 (….).

J. Aerosp. Eng., 2006, 19(4): 217-226

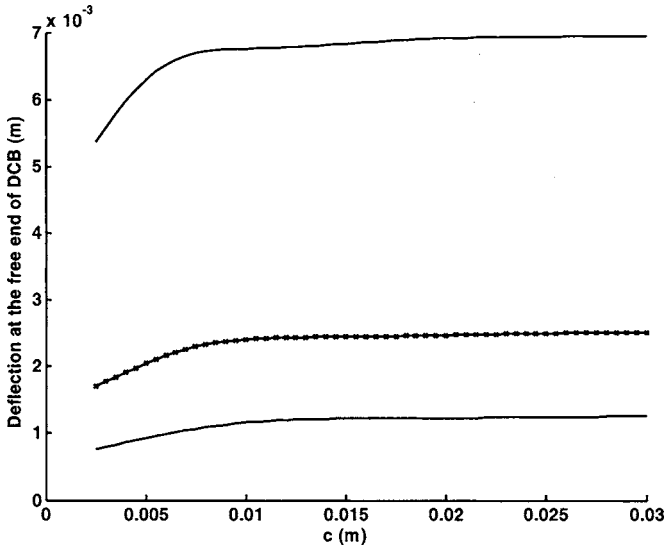

Fig. 14. Effect of length of stitched section and thickness of DCB on deflections of free end of partially stitched *a* graphite/epon DCB. Applied force is 200 N, stiffness of foundation is equal to $k=10^9$ N/m^2. Length of unstitched section of DCB is 30 mm. Thickness of delaminated section is equal to 2 mm (solid curve), 3 mm (-x-x-x-), and 4 mm (….).

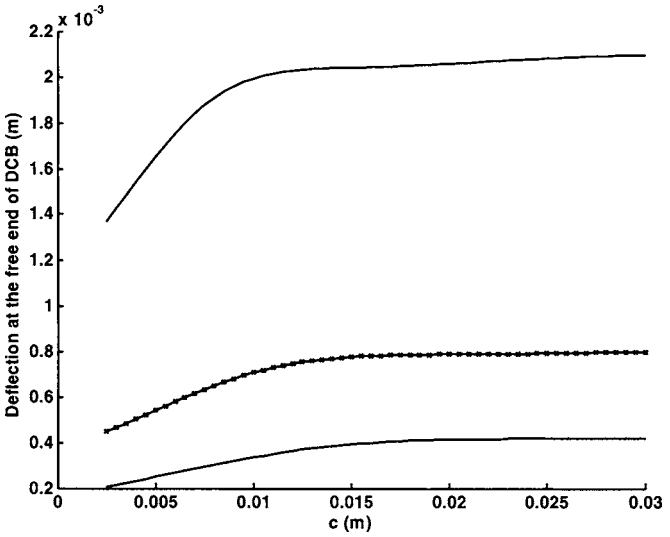

Fig. 15. Effect of length of stitched section and thickness of DCB on deflections of free end of partially stitched *a* unidirectional AS4-3501-6 laminated DCB. Applied force is 200 N, stiffness of foundation is equal to $k=10^9$ N/m^2. Length of unstitched section of DCB is 30 mm. Thickness of delaminated section is equal to 2 mm (solid curve), 3 mm (-x-x-x-), and 4 mm (….).

Maximum bending stresses in delaminated legs of DCB can be evaluated using the present solution. In numerical examples, the maximum stresses in DCB found at the cross section of the first row of stitches were within 15% of the values determined by assumption that the delaminated section of the beam was clamped at this cross section. These stresses were only slightly affected by the stiffness of the elastic foundation, except for very lightly supported stitched sections. The stresses increased almost proportionally to the length of the unstitched delaminated section of DCB from 0.27 to 0.41 GPa as this length varied from 20 to 30 mm. For comparison, the tensile and compressive strengths of a unidirectional AS-3501-6 are 1.45 and 1.18 GPa, respectively (Gibson 1994). Therefore, although bending failure of DCB does not occur in the examples considered here, the maximum stress is of the same order as the strength of the material. This observation is in agreement with the comments in the paper of Ghen et al. (2001) that failure of DCB with a relatively high stitch volume fraction occurs as a result of failure of delaminated sections, rather than the failure of stitches.

Finally, the influence of the thickness of DCB on the deflections of the free end of the delaminated section is illustrated in Figs. 14 and 15. As follows from these figures the thickness of the delaminated leg of DCB may affect the length of the crack penetration into the stitched region corresponding to the arrest of the crack. This is particularly noticeable in Fig. 15 where the crack is arrested at the values of c close to 10, 15, and over 20 mm at thicknesses equal to 2, 3, and 4 mm, respectively (at these penetrations, the curves become horizontal, i.e., an increment in the length crack does not result in a larger crack opening signifying the crack arrest).

Conclusions

The paper represents the analysis of the effectiveness of partially stitched laminates on the example of a double cantilever beam with a delamination crack. While the advantages of stitched composites in the structures where delamination represents a potential mode of failure have been known for a long time, the present solution concentrates on laminates with localized stitching (functionally graded stitched composites). In such laminates, rows of stitches are strategically located across the path of delamination cracks to arrest these cracks before they produce a dangerous damage to the structure.

Double cantilever beams considered in the paper have a pre-existing delamination crack that penetrated into the stitched region. One of the possible modes of damage is failure of the external row of stitches that will typically result in the consecutive failure of adjacent rows of stitches and failure of the entire structure. The other mode of failure is the loss of strength of the delaminated section of the structure. Finally, the crack may continue its propagation, emerge from the stitched region, and unzip the structure. Numerical analysis presented in the paper enables us to assess these modes of failure. The criterion of delamination failure employed in this analysis is based on the evaluation of the rate of change of the characteristic crack opening with the length of the crack. The crack is assumed arrested if this rate becomes equal to zero, i.e., if a longer crack does not correspond to a larger crack opening. The paper presents both static as well as dynamic solutions that can be used to evaluate the effectiveness of partial stitching in the prevention of both static delamination fracture as well as fatigue damage.

As follows from numerical examples presented for the static problem, both the failure of stitches as well as the loss of strength of the delaminated section are possible for geometries and materials considered. However, it is evident that a very significant enhancement of the delamination resistance can be achieved using rows of stitches located across the path of the crack. This approach may be more useful than conventional stitched laminates since the degradation of in-plane strength and stiffness is limited to stitched sections of functionally graded stitched composites. The solution considered on the example of a repre-

J. Aerosp. Eng., 2006, 19(4): 217-226

sentative DCB justifies further studies of more realistic structures to establish the optimum spacing between the rows of stitches and prevents failure.

As follows from numerical examples, if the density of stitches and/or their stiffness increase, the crack is arrested, even if the stitched section is narrow. However, the loss of strength of the delaminated and unsupported section of DCB or the loss of strength of the stitches may become a dominant mode of failure. An optimized solution could be considered using a variable stitch volume fraction in different parts of the structure. A lower stitch volume fraction could be applied in the parts where the retention of in-plane strength and stiffness is critical, while a higher volume fraction of stitches used in other parts of the structure would guarantee the arrest of delamination cracks, even if they form in weakly stitched regions. It is evident that partial stitching of laminated structures, i.e., functionally graded stitched structures, may offer an acceptable compromise between fully stitched and unstitched designs.

Acknowledgments

This research was supported by the U.S. Air Force Office for Scientific Research, Contract No. F33615-98-D-3210.

Notation

The following symbols are used in this paper:

- b = width of DCB;
- EI = Effective bending stiffness of delaminated leg of DCB;
- E_s = modulus of elasticity of stitches;
- GA = shear stiffness of delaminated leg of DCB (product of effective shear modulus and cross-sectional area);
- h = depth of delaminated leg of DCB;
- K = coefficient of elastic clamping (rotational restraint) of intact part of DCB;
- k = coefficient of elastic support provided by stitches to delaminated leg of DCB;
- L = length of one stitch;
- $M(x)$ = bending moment in delaminated leg of DCB;
- P = force applied to delaminated legs of DCB (Fig. 2);
- r = radius of stitches;
- $V(x)$ = transverse shear force acting in delaminated leg of DCB;
- V_p = volume fraction of stitches (it is equal to areal density if stitches are through entire depth of laminate);
- W_i = amplitude of vibrations of delaminated ith leg of DCB;
- w = deflection of delaminated leg of DCB;
- w_b = deflection of delaminated leg of DCB attributed to bending;
- w_s = deflection of delaminated leg of DCB attributed to shear;
- ρ = material mass density of DCB;
- σ_{crit} = strength of stitches;
- τ = interfacial shear strength between stitch and laminate;
- ϕ = rotation of transverse normal as result of deformation;
- Φ_i = amplitude of rotation of normal to middle axis of delaminated ith leg of DCB; and
- ω = frequency of dynamic loading.

References

Barbero, E. J. (1999). *Introduction to composite materials design*, Taylor and Francis, Philadelphia.

Birman, V., and Byrd, L. W. (2005). "Effect of z-pins on fracture in composite cocured double cantilever beams." *J. Aerosp. Eng.*, 18(1), 51–59.

Chen, L., Ifju, P. G., and Sankar, B. V. (2001). "A novel double cantilever beam test for stitched composite laminates." *J. Compos. Mater.*, 35(13), 1137–1149.

Chen, L., Sankar, B. V., and Ifju, P. G. (2003). "Mixed mode fracture toughness tests for stitched composite laminates." *AIAA Pap.*, 2003, 1874.

Dexter, H. B., and Funk, J. G. (1986). "Impact resistance and interlaminar fracture toughness of through-the-thickness reinforced graphite/epoxy." *Proc., 27th AIAA/ASME/ASCE/AHS/ASC Structural Dynamics and Materials Conf.*, AIAA Paper 86-1020, 700–709.

Dow, M., and Dexter, H. B. (1997). "Development of stitched, braided and woven composite structures in the ACT program and at Langley Research Center (1985 to 1997)." *NASA TP 97-206234*, NASA, Washington, D.C.

Dransfield, K., Baillie, C., and Mai, Y.-Y. W. (1994). "Improving the delamination resistance of CFRP by stitching—A review." *Compos. Sci. Technol.*, 50, 305–317.

Dransfield, K., Jain, L. K., and Mai, Y.-W. (1998). "On the effects of stitching in CFRPs—I: Mode I. Delamination toughness." *Compos. Sci. Technol.*, 58(6), 815–827.

Farley, G. L., Smith, B. T., and Maiden, J. L. (1992). "Compression response of thick layer composite laminates with through-the-thickness reinforcements." *J. Reinf. Plast. Compos.*, 11(7), 787–810.

Ghate, V., La Saponare, V., Singh, P., and Whitman, Z. (2004). "Buckling and face wrinkling of stitched sandwich panels." *Proc., Technical Meeting of the Society for the Advancement of Material and Process Engineering* (CD-ROM).

Gibson, R. F. (1994). *Principles of composite material mechanics*, McGraw–Hill, New York.

Gui, L., and Li, Z. (2001). "Delamination buckling of stitched laminates." *Compos. Sci. Technol.*, 61, 629–636.

Jain, L. K., and Mai, Y. W. (1994). "On the effect of stitching on Mode I delamination toughness of laminated composites." *Compos. Sci. Technol.*, 51, 331–345.

Jegley, D. C., Bush, H. G., and Lovejoy, A. E. (2001). "Structural response and failure of a full-scale stitched graphite-epoxy wing." *AIAA Pap.*, 2001, 1334.

Kanninen, M. F. (1973). "An augmented double cantilever beam model for studying crack propagation and arrest." *Int. J. Fract.*, 9, 83–92.

Korotkin, Ya. I., Postnov, V. A., and Sivers, N. L. (1968). *Mechanics of ship structures and theory of elasticity*, Vol. 1, Shipbuilding Publishers, Leningrad, Russia (in Russian).

Lau, K., Ling, H., and Zhou, L. (2004). "Low velocity impact on shape memory alloy stitched composite plates." *Smart Mater. Struct.*, 13, 364–370.

Mabson, G. E., and Deobald, L. R. (2000). "Design curves for 3D reinforced composite laminated double cantilever beams." *Mechanics of sandwich structures*, Y. D. S. Rajapakse, G. A. Kardomateas, and V. Birman, eds., ASME, New York, 89–99.

Ozdil, F., and Carlsson, L. (1999). "Beam analysis of angle-ply laminate DCB specimens." *Compos. Sci. Technol.*, 59, 305–315.

Reddy, J. N. (2004). *Mechanics of laminated composite plates and shells. Theory and analysis*, CRC, Boca Raton, Fla.

Reeder, J. R. (1995). "Stitching vs. a toughened matrix: Compression strength effects." *J. Compos. Mater.*, 29(18), 2464–2487.

Sankar, B. V., and Sharma, S. (1995). "Effects of stitching on fracture toughness of uniweave textile graphite/epoxy laminates." *NASA CP-3311*, Part 2, NASA, Washington, D.C., 481–507.

Whitney, J. M. (1987). *Structural analysis of laminated anisotropic*

plates, Technomic, Lancaster, Pa.
Williams, J. G. (1989). "End correction for orthotropic DCB specimens." *Compos. Sci. Technol.*, 35, 367.
Yavari, A., Sarkani, S., and Reddy, J. N. (2001). "Generalized solutions of beams with jump discontinuities on elastic foundations." *Arch. Appl. Mech.*, 71, 625–639.
Yavuz, A. K., Papoulia, K. D., Phoenix, S. L., and Hui, C. Y. (2005). "Stability analysis of stitched composite plate system with delamination under hydro-thermal pressure." *AIAA Pap.*, 2005, 2106.
Yeh, H. Y., Lee, J. J., and Yang, D. Y. T. (2004). "Study of stitched and unstitched composite panels under shear loadings." *J. Aircr.*, 41, 386–392.

J. Aerosp. Eng., 2006, 19(4): 217-226